

9-22-2004

# Statistical Mechanics of Worm-Like Polymers from a New Generating Function

Gustavo A. Carri

*University of Akron Main Campus, gac@uakron.edu*

Marcelo Marucho

Please take a moment to share how this work helps you [through this survey](#). Your feedback will be important as we plan further development of our repository.

Follow this and additional works at: [http://ideaexchange.uakron.edu/polymer\\_ideas](http://ideaexchange.uakron.edu/polymer_ideas)



Part of the [Polymer Science Commons](#)

---

## Recommended Citation

Carri, Gustavo A. and Marucho, Marcelo, "Statistical Mechanics of Worm-Like Polymers from a New Generating Function" (2004). *College of Polymer Science and Polymer Engineering*. 6.

[http://ideaexchange.uakron.edu/polymer\\_ideas/6](http://ideaexchange.uakron.edu/polymer_ideas/6)

This Article is brought to you for free and open access by IdeaExchange@UAkron, the institutional repository of The University of Akron in Akron, Ohio, USA. It has been accepted for inclusion in College of Polymer Science and Polymer Engineering by an authorized administrator of IdeaExchange@UAkron. For more information, please contact [mjon@uakron.edu](mailto:mjon@uakron.edu), [uapress@uakron.edu](mailto:uapress@uakron.edu).

# Statistical mechanics of worm-like polymers from a new generating function

Gustavo A. Carri<sup>a)</sup> and Marcelo Marucho

*The Maurice Morton Institute of Polymer Science, The University of Akron, Akron, Ohio 44325-3909*

(Received 16 April 2004; accepted 28 June 2004)

We present a mathematical approach to the worm-like chain model of semiflexible polymers. Our method is built on a novel generating function from which all the properties of the model can be derived. Moreover, this approach satisfies the local inextensibility constraint exactly. In this paper, we focus on the lowest order contribution to the generating function and derive explicit analytical expressions for the characteristic function, polymer propagator, single chain structure factor, and mean square end-to-end distance. These analytical expressions are valid for polymers with any degree of stiffness and contour length. We find that our calculations are able to capture the fully flexible and infinitely stiff limits of the aforementioned quantities exactly while providing a smooth and approximate crossover behavior for intermediate values of the stiffness of the polymer backbone. In addition, our results are in very good quantitative agreement with the exact and approximate results of five other treatments of semiflexible polymers. © 2004 American Institute of Physics. [DOI: 10.1063/1.1784771]

## I. INTRODUCTION

Since the ground-breaking ideas introduced by Kratky and Porod in 1949,<sup>1</sup> theoretical studies of semiflexible polymers based on the Kratky–Porod (KP) model, called worm-like polymers henceforth, have been abundant. In this model, the polymer chain displays resistance to bending deformations. The degree of resistance is determined by a free energy that penalizes the different configurations of the chain based on the extent of bending of the polymer backbone. This free energy depends on parameters (elastic constants) that are the result of many short-range monomer-monomer interactions. Explicitly, for the continuous version of the KP model,<sup>2</sup> called the worm-like chain (WLC) model which is the only model for semiflexible polymers studied in this paper, the free energy is

$$H = \frac{\epsilon}{2} \int_0^L ds \left( \frac{\partial \mathbf{R}}{\partial s} \right)^2, \quad (1)$$

where  $\mathbf{R}(s)$  is the vectorial field in three dimensions that represents the polymer chain,  $s$  is the arc of length parameter,  $L$  is the contour length of the polymer, and  $\epsilon$  is the ratio between the bending modulus and the thermal energy. In addition, the local inextensibility constraint  $|d\mathbf{R}(s)/ds|=1$  must be satisfied for all values of the arc of length parameter.

As a consequence of the bending rigidity, a worm-like chain is characterized by a persistence length that is proportional to the bending modulus such that for length scales shorter than the persistence length the chain behaves like a rod while, for length scales larger than the persistence length the chain is governed by the configurational entropy that favors the random-walk conformations.

The local inextensibility constraint has not allowed researchers to find an exact solution to the model when the effects of an external field are added to the theory (see p. 44 in Ref. 3 and, Secs. 15.9.3 and 15.9.1 in Ref. 4). Indeed, the constraint  $|d\mathbf{R}(s)/ds|=1$  is written using a Dirac  $\delta$  distribution in infinite dimensions. Depending on how the constraint is written,  $|d\mathbf{R}(s)/ds|=1$  or  $[d\mathbf{R}(s)/ds]^2=1$ , we obtain path integral representations for the different statistical quantities (e.g., characteristic function) with actions that are nonanalytic or nonlinear, respectively. Consequently, there is no exact solution for the WLC model with an external field at present. However, the path integral representation of the WLC model without an external field is the same one that describes the Brownian motion of a point particle of mass  $\epsilon$  moving on the unit sphere. Since this problem is exactly solvable many properties of the WLC model such as some correlation functions and the first few moments of the distribution of the end-to-end distance are known exactly;<sup>2,3</sup> higher order moments can also be computed exactly using a recursive solution to Schrödinger's equation.<sup>4</sup> However, exact expressions for the different distribution functions are not available at present.

Indeed, many researchers have addressed the WLC model and other models of semiflexible polymers like the model of Dirac chains developed by Kholodenko<sup>5</sup> with the purpose of understanding the statistical behavior of this kind of polymers. Among the many theoretical treatments of worm-like polymers, let us start with two very important contributions made in 1950s: first, the work by Daniels<sup>6</sup> who developed expansions of the polymer propagator for a worm-like polymer in inverse powers of the number of segments and, second, the classic paper by Benoit and Doty<sup>7</sup> where the exact expressions of the mean square end-to-end distance and radius of gyration were obtained. During the following two decades, the field of statistical mechanics of worm-like

<sup>a)</sup> Author to whom any correspondence should be addressed. Electronic mail: gac@uakron.edu

polymers saw a substantial growth, thanks to the seminal contributions of many researchers. For example, Fixman and Kovacs developed a modified Gaussian model for stiff polymer chains under an external field (external force).<sup>8</sup> In this approach, they computed an approximate distribution for the bond vectors from which they were able to compute the partition function and average end-to-end vector. An alternative approach was proposed by Harris and Hearst<sup>9</sup> who developed a distribution for the continuous model from which they were able to compute the two-point correlation function and, consequently, the mean square end-to-end distance and radius of gyration. A reformulation of the KP model using field-theoretic methods was developed by Saitô and co-workers,<sup>2</sup> who computed exactly different averages of the end-to-end distance and tangent-tangent correlation function. In addition, Gobush and co-workers<sup>10</sup> developed an asymptotic expression for the polymer propagator in inverse powers of the number of segments and, Yamakawa and Stockmayer<sup>11</sup> addressed the first order correction to the mean square end-to-end distance and second virial coefficient due to excluded volume interactions. Other seminal contributions to the understanding of the WLC model made by Yamakawa and collaborators have been summarized in Ref. 3 recently. Worm-like polymers were also studied using field-theoretic methods by Freed<sup>12</sup> who developed a modified Gaussian distribution approximation for the WLC model.<sup>13</sup> This distribution has been rederived using different mathematical methods by Lagowski and co-workers,<sup>14</sup> and Winkler *et al.*<sup>15</sup> Similar results were obtained by Zhao and collaborators<sup>16</sup> who also studied the effect of an external field. Field-theoretic methods have also been used by Bhattacharjee and Muthukumar<sup>17</sup> who employed the Edwards-Singh self-consistent approach to obtain an effective Gaussian Hamiltonian which they used to compute the mean square end-to-end distance.

In recent years, the advent of new experimental methods that have allowed researchers to manipulate single molecules has generated new momentum in the area of statistical mechanics of worm-like polymers.<sup>18</sup> Indeed, new analytical and numerical approaches to worm-like polymers have been developed by Marko and Siggia, Kroy and Frey, and Samuel and Sinha<sup>19</sup> who derived the force-elongation relationship predicted by the WLC model, Hansen and Podgornik<sup>20</sup> who developed a nonperturbative  $1/d$  expansion ( $d$  being the dimension of the embedding space), Wilhelm and Frey<sup>21</sup> who computed the polymer propagator for polymers with large bending rigidities, Winkler<sup>22</sup> who computed the same quantity for any value of the stiffness of the polymer backbone using the maximum entropy principle, and Kleinert<sup>4</sup> who developed a recursive solution to Schrödinger's equation from where the all the moments of the polymer propagator can be calculated exactly. Kleinert has also proposed a particular mathematical expression for the polymer propagator. More recently, Stepanow and Schütz<sup>23</sup> computed the Fourier-Laplace transform of the polymer propagator systematically by mapping the WLC model onto the problem of random walks with constraints, which is related to the representation theory of the Temperley-Lieb algebra.

The WLC model is not the only description of semiflex-

ible polymers available in the literature. Indeed, other models for semiflexible polymers have been developed. Among these other approaches it is important for the purposes of this paper to mention the model of Dirac chains developed by Kholodenko.<sup>5</sup> The advantage of this model is that statistical quantities such as the force-elongation relationship and single chain structure factor can be calculated *exactly* and, moreover, have been used to describe experimental data and compare well with approximate results of the WLC model. The origin of the quantitative agreement between the different observables of both models can be found in the approximate equivalence between the WLC model and the model of Dirac chains. This was proved by Kholodenko using the Bloch-Nordsieck approximation. The approximate equivalence between both models and the availability of an exact solution for the model of Dirac chains make this model very useful for the purpose of estimating the quality of our approximations for the WLC model.<sup>5</sup>

In this paper we revisit the WLC model of semiflexible polymers with the purpose of developing a new approximate method capable of providing closed form expressions for the most commonly studied statistical properties of the model. The main motivation for this study is to obtain these expressions from a unique approximation to the model such that these expressions are accurate for any value of the persistence length. Since all these results are obtained from a single approximate treatment of the model, they are on equal footing. In other words, we do not have to develop different approximations for different statistical quantities or regimes with different degrees of stiffness. This feature is one important advantage of this work. We show in this article that some statistical quantities (e.g., the polymer propagator in real space) are described by very simple and accurate mathematical formulas when our method is employed. However, the consequences of the approximate nature of our method appear in two parameters that our calculation cannot predict at present therefore, they are determined *a posteriori* by comparing our results with the ones obtained by other approximate treatments of the WLC model. Although this lack of self-consistency is the most important drawback of our calculation, it is also one of its major strengths since it allows us to connect our method with the results obtained by other research groups.

Let us be more explicit about the objectives of this work. Our main objective is to find a solution to the WLC model capable of reproducing the statistical properties of the model approximately. Furthermore, we require that our solution captures all the statistical properties of the rod-like and flexible limits exactly. Moreover, our solution must respect the local, not global, inextensibility constraint. In the crossover region, the solution is not exact but, we require that it displays the correct physical features as described by other approximate and exact descriptions of semiflexible polymers. Finally, our solution should be amenable to systematic and controlled corrections calculated in a perturbative manner. In this paper, we only provide the guidelines for the development of such perturbation expansion but leave the detailed mathematical calculations for a future article where we will also address the excluded volume problem.

This article is organized as follows. In Sec. II, we start with the KP model and propose a generating function that we evaluate approximately. This section also contains the continuous limit (WLC model) and the two approximations required by our calculation together with their justifications. Afterward, we use the generating function to calculate the characteristic function, mean square end-to-end distance, polymer propagator, and single chain structure factor of the model. In Sec. III we discuss the results of our calculations which are valid for any value of the stiffness of the polymer backbone and length of the polymer chain. Moreover, for the purpose of making our presentation more balanced and objective, we present a quantitative comparison of our results with those obtained by other researchers using different descriptions of semiflexible polymers (Dirac chains) and different approximations to the WLC model. Sec. IV contains the conclusions of our work. The details of some mathematical calculations are presented in the Appendix.

## II. THEORY

### A. Review of the Kratky–Porod model and the generating function

Let us consider a polymer chain as a set of  $n$  bond vectors ( $\mathbf{u}_0, \mathbf{u}_1, \dots, \mathbf{u}_{n-1}$ ) connected in a sequential manner. Furthermore, let us assume that the length of each bond vector is  $l_k$  (=Kuhn length) and that pairs of consecutive bond vectors try to be parallel to each other. This orientational interaction is modeled with a Boltzmann weight given by the following mathematical expression<sup>8,17</sup>

$$\exp\left(-\frac{\epsilon}{2l_k^2 k_B T} \sum_{k=0}^{n-2} (\mathbf{u}_{k+1} - \mathbf{u}_k)^2\right), \quad (2)$$

where  $\epsilon$  and  $k_B T$  are the bending and thermal energies, respectively. In addition, we take into account the local inextensibility constraint with the following term:<sup>2</sup>

$$\prod_{i=0}^{n-1} \delta\left(\frac{(\mathbf{u}_i)^2}{l_k^2} - 1\right). \quad (3)$$

The expressions given by Eqs. (2) and (3) define the KP model completely and all the statistical properties of the model such as the characteristic function, single chain structure factor and other correlation functions, probability distributions like the polymer propagator and their moments can be calculated. The evaluation of these statistical properties can be easily done using the following generating function:

$$C(\{\Psi_{kjp}\}) \equiv \left\langle \exp\left(\sum_{k=0}^{n-1} \mathbf{u}_k \cdot \Psi_{kjp}\right) \right\rangle, \quad (4)$$

where  $\Psi_{kjp}$  is defined as follows:

$$\Psi_{kjp} \equiv \mathbf{J}_k + i\mathbf{q} \cdot [\Theta(k-j) - \Theta(k-p)]. \quad (5)$$

This definition shows that  $\Psi_{kjp}$  is an auxiliary tensor. It represents a standard external source consisting of two terms, the first one,  $\mathbf{J}_k$ , represents a dipolar coupling with the  $k$ th bond vector and, the second one,  $\mathbf{q}$ , is also a dipolar coupling

that is nonzero only when the  $k$ th bond vector is located between the  $j$ th and  $p$ th ones along the polymer chain.  $\Theta(z)$  is the Heaviside step function.<sup>24</sup>

If the generating function defined in Eq. (4) is known, then all the aforementioned statistical properties can be obtained from it by differentiation with respect to  $\{\mathbf{J}_k\}$  and/or by assigning specific values to  $\{\mathbf{J}_k\}$ . For example, the characteristic function is obtained from Eq. (4) by setting all the  $\mathbf{J}_k$  variables equal to zero,  $C\{i\mathbf{q} \cdot [\Theta(k-j) - \Theta(k-p)]\}$ ; the polymer propagator is the inverse Fourier transform of the characteristic function  $C(i\mathbf{q})$  and the tangent-tangent correlation function,  $\langle \mathbf{u}_j \cdot \mathbf{u}_k \rangle$ , is computed as the second-order derivative of the generating function with respect to  $\mathbf{J}_j$  and  $\mathbf{J}_k$ , afterward, this result should be evaluated for values of  $\{\mathbf{J}_k\}$  equal to zero. Other statistical quantities can also be computed easily. Consequently, our first step is to evaluate  $C(\{\Psi_{kjp}\})$  whose explicit mathematical expression is

$$C(\{\Psi_{kjp}\}) = \frac{1}{z} \int \left[ \prod_{i=0}^{n-1} d\mathbf{u}_i \delta\left(\frac{(\mathbf{u}_i)^2}{l_k^2} - 1\right) \right] \times \exp\left\{-\frac{\epsilon}{2l_k^2 k_B T} \sum_{k=0}^{n-2} (\mathbf{u}_{k+1} - \mathbf{u}_k)^2 + \sum_{k=0}^{n-1} \mathbf{u}_k \cdot \Psi_{kjp}\right\}, \quad (6)$$

where  $z$  is defined in such a way that  $C(\{\mathbf{0}_{kjp}\}) = 1$ . We now rewrite the  $\delta$  distributions in Eq. (6) as follows:

$$\prod_{j=0}^{n-1} \delta\left(\frac{(\mathbf{u}_j)^2}{l_k^2} - 1\right) = \prod_{j=0}^{n-1} \frac{l_k^3}{(2\pi)^2} \int d\Phi_j \frac{\cos(\Phi_j l_k)}{(\Phi_j l_k)^2} \hat{\mathcal{O}}_1(\lambda_j) \times \left[ \exp\left(i l_k \Phi_j \cdot \frac{\mathbf{u}_j}{l_k} (1 + \lambda_j)\right) \right], \quad (7)$$

where  $\hat{\mathcal{O}}_i(\lambda_j)[\dots]$  is an operator whose function is to take the first  $i$  terms of the Taylor series in powers of  $\lambda_j$  of the argument and evaluate this result for  $\lambda_j = 1$ .

After replacing the  $\delta$  distributions in Eq. (6) with the integral representations described in Eq. (7) the mathematical expression for the generating function becomes

$$C(\{\Psi_{kjp}\}) = \frac{1}{z} \int \left[ \prod_{q=0}^{n-1} d\mathbf{u}_q d\Phi_q \frac{\cos(\Phi_q l_k)}{(\Phi_q l_k)^2} \hat{\mathcal{O}}_1(\lambda_q) \right] \times \left\{ \exp\left[-\frac{\epsilon}{2l_k^2 k_B T} \sum_{k=0}^{n-2} (\mathbf{u}_{k+1} - \mathbf{u}_k)^2 + \sum_{k=0}^{n-1} \mathbf{u}_k \cdot [\Psi_{kjp} + i\Phi_k (1 + \lambda_k)]\right] \right\}. \quad (8)$$

The integrals over the variables  $\mathbf{u}_k$  are evaluated exactly using the saddle point method. The mathematical expression for the saddle point is the following

$$\mathbf{u}_k = \mathbf{u}_0 - \frac{l_k^2 k_B T}{\epsilon} \sum_{m=0}^{k-1} [\Psi_{mj} + i\Phi_m (1 + \lambda_m)] (k - m). \quad (9)$$

In addition, the following constraint must be fulfilled:

$$\sum_{m=0}^{n-1} [i\Phi_m(1+\lambda_m) + \Psi_{mjp}] = 0. \quad (10)$$

After we replace the expression for the saddle point given by Eq. (9) into the expression for the generating function given by Eq. (8) and writing the constraint, Eq. (10), using the exponential representation of the delta distribution, the expression of the generating function becomes

$$C(\{\Psi_{kjp}\}) = \frac{1}{z} \int d\mathbf{u} \left\{ \int \left[ \prod_{q=0}^{n-1} d\Phi_q \frac{\cos(l_k|\Phi_j|)}{(l_k|\Phi_j|)^2} \hat{O}_1(\lambda_q) \right] \times \exp \left[ i \sum_{s=0}^{n-1} \mathbf{u} \cdot [\Phi_s(1+\lambda_s) - i\Psi_{sjp}] \right] - \frac{\kappa n}{2} \sum_{k=0}^{n-1} \sum_{s=0}^{n-1} [i\Phi_k(1+\lambda_k) + \Psi_{kjp}] K_{k,s} [i\Phi_s(1+\lambda_s) + \Psi_{sjp}] \right\}, \quad (11)$$

where the kernel  $K_{k,s}$  and the parameter  $\kappa$  are defined as follows:

$$K_{k,s} \equiv \left[ 1 - \frac{k}{n} - \frac{\Theta(s-k)}{n} (s-k) \right] \quad \text{and} \quad \kappa \equiv \frac{l_k^2 k_B T}{\epsilon}. \quad (12)$$

We refer the reader to Appendix for some mathematical details of this part of the calculation.

Another mathematical expression for the kernel  $K_{k,s}$  is

$$\left[ \left( 1 - \frac{k+s}{2n} \right) - \frac{|s-k|}{2n} \right].$$

Note that the contribution to double integral arising from the term  $[1 - (k+s)/2n]$  in the kernel vanishes due to the constraint depicted by Eq. (10). Therefore, we remove these contributions from the definition of the kernel  $K_{k,s}$  henceforth. Then, the generating function can be written as follows:

$$C(\{\Psi_{kjp}\}) = \frac{1}{z} \int d\mathbf{u} \left\{ \int \left[ \prod_{q=0}^{n-1} d\Phi_q \frac{\cos(l_k|\Phi_j|)}{(l_k|\Phi_j|)^2} \hat{O}_1(\lambda_q) \right] \times \left[ \exp \left[ i \sum_{s=0}^{n-1} \mathbf{u} \cdot [\Phi_s(1+\lambda_s) - i\Psi_{sjp}] \right] - \frac{\kappa n}{4} \sum_{k=0}^{n-1} \sum_{s=0}^{n-1} [\Phi_k(1+\lambda_k) - i\Psi_{kjp}] \frac{|s-k|}{n} [\Phi_s(1+\lambda_s) - i\Psi_{sjp}] \right] \right\}. \quad (13)$$

The next step involves the integration over the variables  $\Phi_q$ . These integrals cannot be evaluated exactly because the kernel generates *nonlocal* correlations between the variables. In other words, the variable  $\Phi_s$  is correlated to  $\Phi_j$  where  $j \neq s$ . These nonlocal correlations make the exact evaluation of the integrals in Eq. (13) impossible and force us to search for an approximate method to evaluate them. First, we observe that the term containing the cosine function inside the product cannot be approximated and must be kept intact.

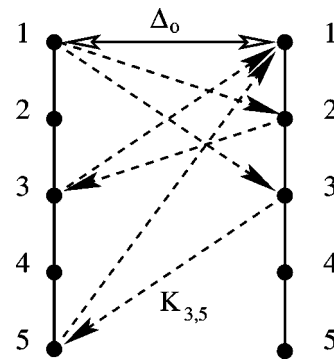


FIG. 1. Illustration of the definition of the effective self-correlation,  $\Delta_o$  (continuous line), in terms of the correlations propagated by the kernel  $K_{k,s}$  (dashed line). Only two paths are showed. Both vertical lines represent the *same* polymer. Numbers indicate the variables along the polymer chain.

Otherwise, the local inextensibility constraint would be violated and the model would lead to the Gaussian chain model. A similar argument can be made for the first term in the exponential of Eq. (13). If this term is approximated, then the exact results of the flexible and rigid limits are lost. Since our approach must capture these two limits exactly and preserve the local inextensibility constraint intact then, the only term that we are allowed to approximate is the second term in the exponential. Moreover, the only quantity that we can approximate in the second term such that we can evaluate the  $\Phi_q$  integrals is the nonlocal kernel.

Let us study the second term in the exponential of Eq. (13). Observe that the nonlocal kernel correlates the behavior of the  $j$ th variable with the behaviors of all the *other* variables. In other words, there is no self-correlation (correlation of  $\Phi_q$  with itself). Thus, we can represent these correlations with a diagram shown in Fig. 1. The vertical lines represent the *same* polymer chain. We show two lines to clarify how the different variables *on the same polymer* correlate with each other. The dashed lines represent the correlations between pairs of variables that are propagated by the kernel  $K_{k,s}$ . Since  $K_{k,s}$  does not allow self-correlations, variables with the same value of the subindex are not correlated via the kernel  $K_{k,s}$ . However, there are paths that lead to *effective* self-correlations. One example of this is the case where the first variable is correlated with the second one, the second one with the third one and this one with the first one. Another possible path for the self-correlation would be the first variable correlating with the third one, the third one with the fifth one and this one with the first one. Clearly, other paths can be constructed. The addition of *all* these paths defines an effective self-correlation for the first variable. We call this self-correlation  $\Delta_o$ . Similarly, this self-correlation can be defined for all other variables along the polymer chain. We assume that this self-correlation is independent of the position of the variable along the polymer chain but depends only on the length of the polymer and its stiffness. In addition, if we could sum the contributions from all the paths, then we would be able to compute  $\Delta_o$  directly from the model. Unfortunately, this is equivalent to solve the model exactly which is not possible at present. Thus,  $\Delta_o$  is left as an adjustable parameter to be determined *a posteriori* by an

appropriate criterion. Using the concept of effective self-correlation, we approximate the kernel as follows:

$$K_{k,s} \approx \frac{1}{2} \Delta_o(\kappa/l_k, nl_k) \delta_{ks}, \quad (14)$$

where  $\delta_{ks}$  is Kronecker's delta.

At this point it is relevant to analyze the consequences of this first approximation. Observe that the replacement of  $K_{k,s}$  by a diagonal term implies that the internal correlations are taken into account on an average sense. Thus, this lowest level of approximation for our generating function cannot describe correlation functions like  $\langle \mathbf{u}_j \cdot \mathbf{u}_k \rangle$  accurately. Another important quantity that is affected by this first approximation is the single chain structure factor. However, we will show that the consequences of this approximation on the structure factor are negligible.

It is worth mentioning that the results obtained using the approximation mentioned in the previous paragraph are amenable to corrections calculated in a controlled manner. One way of improving the accuracy of the results is to take into account the presence of the nearest neighbors explicitly in Eq. (13). This approach is similar to the Bethe approximation for the Ising model and would lead to correlations between nearest neighbor variables,  $\Phi_s$  and  $\Phi_{s+1}$ , via the kernel  $K_{s,s\pm 1}$ . Consequently, another effective correlation,  $\Delta_1(\kappa/l_k, nl_k)$ , would appear in the theory. Further improvements could be made by accounting explicitly for the corre-

lations with nearest neighbors in higher shells. Another method is the perturbative one. In this case we have to add and subtract  $\Delta_o$  to the kernel in Eq. (13) and assume that the contributions arising from the difference between  $\Delta_o$  and the kernel are small. A simple Taylor expansion in powers of the difference between  $\Delta_o$  and the kernel leads to a standard perturbative analysis.

In this paper, we focus on the lowest order contribution to the generating function and postpone the analysis of higher order corrections for a future publication. Using the approximation described before the expression of the generating function given in Eq. (13) can be written as follows:

$$C_o(\{\Psi_{kjp}\}) = \frac{1}{z} \int d\mathbf{u} \left\{ \int \left[ \prod_{q=0}^{n-1} d\Phi_q \frac{\cos(l_k |\Phi_j|)}{(l_k |\Phi_j|)^2} \hat{O}_1(\lambda_q) \right] \times \left[ \exp \left[ i \sum_{s=0}^{n-1} \mathbf{u} \cdot [\Phi_s(1+\lambda_s) - i\Psi_{sjp}] \right] - \frac{\kappa n \Delta_o}{4} \sum_{k=0}^{n-1} [\Phi_k(1+\lambda_q) - i\Psi_{kjp}]^2 \right] \right\}. \quad (15)$$

The evaluation of the integrals over the variables  $\Phi_q$  is simplified by the use of spherical coordinates. The resulting mathematical expression for the generating function is

$$C_o(\{\Psi_{kjp}\}) = \frac{(\pi)^{(2n)}}{z} \int d\mathbf{u} \left\{ \prod_{q=0}^{n-1} \hat{O}_1(\lambda_q) \frac{\exp \left[ \frac{\kappa n \Delta_o}{4} (\Psi_{qjp})^2 + \mathbf{u} \cdot \Psi_{qjp} \right]}{(1+\lambda_q) \left| \frac{\kappa n \Delta_o}{2l_k} \Psi_{qjp} + \frac{\mathbf{u}}{l_k} \right|} \left[ \operatorname{erf} \left( \left[ \frac{1}{(1+\lambda_q)} + \left| \frac{\kappa n \Delta_o}{2l_k} \Psi_{qjp} + \frac{\mathbf{u}}{l_k} \right| \right] \frac{l_k}{\sqrt{\kappa n \Delta_o}} \right) - \operatorname{erf} \left( \left[ \frac{1}{(1+\lambda_q)} - \left| \frac{\kappa n \Delta_o}{2l_k} \Psi_{qjp} + \frac{\mathbf{u}}{l_k} \right| \right] \frac{l_k}{\sqrt{\kappa n \Delta_o}} \right) \right] \right\}. \quad (16)$$

Afterward, we apply the operator  $\hat{O}_1(\lambda_q)$  to the integrand in Eq. (16). As a result, we obtain the following expression for the generating function:

$$C_o(\{\Psi_{kjp}\}) = \frac{1}{z} \int d\mathbf{u} \prod_{q=0}^{n-1} \exp \left( - \frac{u^2}{\kappa n \Delta_o} \right) \times \frac{\sinh \left( \frac{2l_k}{\kappa n \Delta_o} \left| \frac{\kappa n \Delta_o}{2} \Psi_{qjp} + \mathbf{u} \right| \right)}{\frac{2l_k}{\kappa n \Delta_o} \left| \frac{\kappa n \Delta_o}{2} \Psi_{qjp} + \mathbf{u} \right|}, \quad (17)$$

where  $|\dots|$  should be understood as  $\sqrt{(\dots)^2}$ .

Finally, we take the continuous limit of the expression given in Eq. (17) to obtain an expression valid for the WLC

model. For this purpose, we rewrite the parameters of the discrete model in terms of the contour length  $L = nl_k$  and persistence length  $\ell_p = l_k^2/\kappa$  of the chain [i.e.,  $\Delta_o = \Delta_o(L, \ell_p)$ ]. Afterward, we split the product over  $q$  (segments) in Eq. (17) into two products. The first one is the product over all the persistence lengths that can fit in a polymer with contour length  $L$ . The second one is the product over all the segments that can fit in one persistence length. Clearly, this factorization of the product has two implications. First, it assumes that an integer number of segments forms a persistence length and, second, that the polymer has an integer number of persistence lengths. We will explain how to resolve this limitation after presenting the second approximation of our approach. After factorizing the product and rewriting all the parameters in terms of the ones of the continuous model, Eq. (17) becomes

$$C_o(\{\Psi_{kjp}\}) = \frac{1}{z} \int d\mathbf{u} \exp\left(-\frac{u^2 \ell_p}{\Delta_o}\right) \prod_{\alpha=0}^{L/\ell_p} \prod_{q=0}^{\ell_p/l_k} \frac{\sinh\left(\frac{2l_k \ell_p}{L\Delta_o} \left| \frac{L\Delta_o}{2\ell_p} \Psi_{\{\alpha,q\}jp} + \mathbf{u} \right|\right)}{\frac{2l_k \ell_p}{L\Delta_o} \left| \frac{L\Delta_o}{2\ell_p} \Psi_{\{\alpha,q\}jp} + \mathbf{u} \right|}. \quad (18)$$

At this point it is relevant to say that the WLC model does not depend on the Kuhn length,  $l_k$ , explicitly. Indeed, the model depends on two length scales determined by  $\ell_p$  which is the ultraviolet cutoff of the model and  $L$  which represents the infrared cutoff of the theory. If the physical phenomenon of interest has a characteristic length scale shorter than  $\ell_p$ , then the WLC model cannot describe it. For these length scales, the WLC model predicts the behavior of a structureless rigid rod. Consequently, one can naturally assume that the product over the segments inside a persistence length in Eq. (18) can be approximated by the argument of the product where  $l_k$  is replaced by  $\ell_p$ ,

$$\prod_{q=0}^{\ell_p/l_k} \frac{\sinh\left(\frac{2l_k \ell_p}{L\Delta_o} \left| \frac{L\Delta_o}{2\ell_p} \Psi_{\{\alpha,q\}jp} + \mathbf{u} \right|\right)}{\frac{2l_k \ell_p}{L\Delta_o} \left| \frac{L\Delta_o}{2\ell_p} \Psi_{\{\alpha,q\}jp} + \mathbf{u} \right|} \cong \frac{\sinh\left(\frac{2\ell_p^2}{L\Delta_o} \left| \frac{L\Delta_o}{2\ell_p} \Psi_{\alpha jp} + \mathbf{u} \right|\right)}{\frac{2\ell_p^2}{L\Delta_o} \left| \frac{L\Delta_o}{2\ell_p} \Psi_{\alpha jp} + \mathbf{u} \right|}. \quad (19)$$

This is the second approximation of our approach and has two important consequences. On the one hand, this approximation removes  $l_k$  from the model in agreement with the fact that the WLC model does not depend on  $l_k$ . On the other hand, it assumes a specific functional form for the product over  $q$ . This function is exact if one persistence length were to behave like a rigid rod. However, even in the case of very short polymers ( $L \ll \ell_p$ ), some fluctuations with respect to the rigid rod configuration are possible. These fluctuations can be accounted for if we define the ratio  $L/\ell_p$  used in our calculations as a function of the *true* ratio  $L/\ell_p$ . In other words, the fluctuations renormalize the ratio  $L/\ell_p$  of our approach. The functional relationship between the ratio  $L/\ell_p$  used in our calculations and the true one is unknown. Thus, we will construct this relationship later by comparing our results with the ones obtained from other treatments of the WLC model.

Finally, we replace the result obtained in Eq. (19) into the expression of the generating function given by Eq. (18) to obtain the most general expression for the generating function  $C(\{\Psi_{kjp}\})$ ,

$$C_o(\{\Psi_{kjp}\}) = \frac{1}{z} \int d\mathbf{u} \exp\left(-\frac{u^2 \ell_p}{\Delta_o}\right) \times \left[ \frac{\sinh\left(\frac{2\ell_p^2}{L\Delta_o} \left| \frac{L\Delta_o}{2\ell_p} \Psi_{qjp} + \mathbf{u} \right|\right)}{\frac{2\ell_p^2}{L\Delta_o} \left| \frac{L\Delta_o}{2\ell_p} \Psi_{qjp} + \mathbf{u} \right|} \right]^{L/\ell_p}. \quad (20)$$

Observe that the power  $L/\ell_p$  was originally obtained under the assumption that it was an integer number. However, since  $L/\ell_p$  is renormalized by the fluctuations, as discussed before, it can be a real number. Although this does not change the underlying conceptual physics of the approximations, it does have important implications from the computational point of view. If  $L/\ell_p$  is real, then whenever the imaginary part of the ratio

$$\frac{\sinh\left(\frac{2\ell_p^2}{L\Delta_o} \left| \frac{L\Delta_o}{2\ell_p} \Psi_{qjp} + \mathbf{u} \right|\right)}{\frac{2\ell_p^2}{L\Delta_o} \left| \frac{L\Delta_o}{2\ell_p} \Psi_{qjp} + \mathbf{u} \right|}, \quad (21)$$

changes sign, there will be a cut on the complex plane. Crossing these cuts generates discontinuous behavior for the different functions. These discontinuities are artifacts of the extension of our approximations from integer values of  $L/\ell_p$  to real ones. Thus, when using any of the mathematical expressions derived hereafter, we must make sure that they are evaluated on *only one* Riemann sheet so that cuts are avoided.

### B. Characteristic function

Let us start with the evaluation of the characteristic function. This function is obtained from the mathematical expression of the generating function given in Eq. (20) when the external field  $\Psi_{qjp}$  is replaced with  $i\mathbf{q}$  where  $\mathbf{q}$  is the scattering wave vector. Then, the mathematical expression for the characteristic function is

$$C(q) = \frac{1}{2i\ell_p q z} \int_0^{+\infty} du \exp\left(-\frac{u^2 \ell_p}{\Delta_o}\right) \times u \left\{ \int_{2\ell_p^2/L\Delta_o(u-iqL\Delta_o/2\ell_p)}^{2\ell_p^2/L\Delta_o(u+iqL\Delta_o/2\ell_p)} v \left[ \frac{\sinh(v)}{v} \right]^{L/\ell_p} dv \right\}. \quad (22)$$

This expression can be simplified further by an integration by parts over the variable  $u$  and with the help of the following definitions:  $h(z) - \overline{h(z)} = 2i \text{Im}[h(z)]$  and  $h(\overline{z}) = \overline{h(z)}$ , where

$$h(z) = \left( [\sinh(z)]^{L/\ell_p} / [z]^{L/\ell_p - 1} \right).$$

As a result, the expression for the characteristic function becomes

$$C(q) = \frac{1}{qzL} \int_0^{+\infty} du \exp\left(-\frac{u^2 \ell_p}{\Delta_o}\right) \times \text{Im} \left\{ \frac{\left[ \sinh\left[ \frac{2\ell_p^2}{L\Delta_o} \left( u + iq \frac{L\Delta_o}{2\ell_p} \right) \right] \right]^{L/\ell_p}}{\left[ \frac{2\ell_p^2}{L\Delta_o} \left( u + iq \frac{L\Delta_o}{2\ell_p} \right) \right]^{L/\ell_p - 1}} \right\}. \quad (23)$$

Observe that in the limit  $L/\ell_p \rightarrow \infty$  the integral representation of the characteristic function given in Eq. (23) approaches the asymptotic limit given by the formula

$$C_{L/\ell_p \rightarrow \infty}(q) \sim \left[ \frac{\sin(q\ell_p)}{q\ell_p} \right]^{L/\ell_p}, \quad (24)$$

which, if the ratio  $L/\ell_p$  is an integer, is the characteristic function of the random flight model.<sup>25</sup>

On the other hand, in the limit  $L/\ell_p \rightarrow 0$  the characteristic function approaches the rodlike limit<sup>26</sup>

$$C_{L/\ell_p \rightarrow 0}(q) = \frac{\sin(qL)}{qL}. \quad (25)$$

In addition, the expression of the characteristic function given in Eq. (23) has an analytical solution for the entire range of values of  $L/\ell_p$ , which is

---


$$C(q) = \frac{1}{qzL2^{L/\ell_p}} \sum_{p=0}^{\infty} \binom{L/\ell_p}{p} (-)^p \text{Im} \left\{ \int_0^{+\infty} du \frac{\exp\left[ -\frac{u^2 \ell_p}{\Delta_o} + \left( \frac{L}{\ell_p} - 2p \right) \frac{2\ell_p^2}{L\Delta_o} \left( u + iq \frac{L\Delta_o}{2\ell_p} \right) \right]}{\left[ \frac{2\ell_p^2}{L\Delta_o} \left( u + iq \frac{L\Delta_o}{2\ell_p} \right) \right]^{L/\ell_p - 1}} \right\}, \quad (26)$$


---

where we have expanded the function  $\sinh^x(z)$  in powers of  $z$ .<sup>24</sup> This expression for the characteristic function avoids all the cuts introduced by the extension of  $L/\ell_p$  to real values.

### C. Mean square end-to-end distance

We now proceed to evaluate the mean square end-to-end distance  $\langle R^2 \rangle$  and the norm  $z$  from the expansion of the characteristic function in powers of the wave vector. First, we change variables as follows:

$$v = v(x) = \sqrt{\left( \frac{2\ell_p^2}{L\Delta_o} u \right)^2 + 2i \frac{2\ell_p^2}{L\Delta_o} u \ell_p q x - \ell_p^2 q^2},$$

$$u = u(t) = \frac{L\Delta_o}{2\ell_p^2} t, \quad (27)$$

then, the expression of the characteristic function given by Eq. (22) becomes

$$C(q) = \frac{1}{2z} \left[ \frac{L\Delta_o}{2\ell_p^2} \right]^2 \int_0^{+\infty} dt \exp\left[ -\frac{t^2 \Delta_o}{4} \left( \frac{L}{\ell_p} \right)^2 \right] t^2 \times \int_{-1}^1 dx \left( \frac{\sinh(\sqrt{t^2 + 2it\ell_p qx - \ell_p^2 q^2})}{\sqrt{t^2 + 2it\ell_p qx - \ell_p^2 q^2}} \right)^{L/\ell_p}. \quad (28)$$

In the limit of small wave vectors, the integral representation of the characteristic function given in Eq. (28) has the following asymptotic behavior:

$$C(q) = \frac{1}{z} \left[ \frac{L\Delta_o}{2\ell_p^2} \right]^2 \int_0^{+\infty} dt \times \exp\left[ -\frac{t^2 \Delta_o}{4} \left( \frac{L}{\ell_p} \right)^2 \right] t^2 \left\{ \left( \frac{\sinh(t)}{t} \right)^{L/\ell_p} - \frac{L\ell_p q^2 \sinh^{L/\ell_p}(t)}{6t^{L/\ell_p+2}} \left[ \left( \frac{L}{\ell_p} t^2 + \frac{L}{\ell_p} - 1 \right) + \left( \frac{L}{\ell_p} - 1 \right) t[-2 \coth(t) + \text{csch}(t)t] \right] \right\}, \quad (29)$$

where, in order to satisfy the condition  $C(0) = 1$ , we define  $z$  as follows:

$$z = \left[ \frac{L\Delta_o}{2\ell_p^2} \right]^2 A_{L/\ell_p - 2}^{L/\ell_p} \left( \frac{L}{\ell_p}, \frac{\Delta_o}{\ell_p} \right). \quad (30)$$

$A_a^b(L/\ell_p, \Delta_o/\ell_p)$  is defined by the following formula:

$$A_a^b \left( \frac{L}{\ell_p}, \frac{\Delta_o}{\ell_p} \right) = \int_0^{+\infty} dt \exp\left[ -\frac{t^2 \Delta_o}{4} \left( \frac{L}{\ell_p} \right)^2 \right] \frac{\sinh^b(t)}{t^a}. \quad (31)$$

The second-order derivative of the characteristic function with respect to the wave vector evaluated at  $q = 0$  determines the expression of the mean square end-to-end distance. The final expression for  $\langle R^2 \rangle$  is



$$\begin{aligned} \langle R^2 \rangle &= -6 \left. \frac{\partial^2 C(q)}{\partial q^2} \right|_{q=0} \\ &= \frac{L\ell_p}{z} \left[ \frac{L\Delta_o}{2\ell_p^2} \right]^2 \int_0^{+\infty} dt \\ &\quad \times \exp \left[ -\frac{t^2}{4} \frac{\Delta_o}{\ell_p} \left( \frac{L}{\ell_p} \right)^2 \right] \frac{\sinh^{L/\ell_p}(t)}{t^{L/\ell_p}} \left\{ \left( \frac{L}{\ell_p} t^2 + \frac{L}{\ell_p} - 1 \right) \right. \\ &\quad \left. + \left( \frac{L}{\ell_p} - 1 \right) t \left[ -2 \coth(t) + \operatorname{csch}^2(t)t \right] \right\}, \end{aligned} \quad (32)$$

or, in terms of  $A_a^{b(L/\ell_p, \Delta_o/\ell_p)}$ ,

$$\begin{aligned} \langle R^2 \rangle &= \frac{L\ell_p}{A_{L/\ell_p-2}^{L/\ell_p} \left( \frac{L}{\ell_p}, \frac{\Delta_o}{\ell_p} \right)} \left\{ A_{L/\ell_p}^{L/\ell_p} \left( \frac{L}{\ell_p}, \frac{\Delta_o}{\ell_p} \right) \left( \frac{L}{\ell_p} - 1 \right) \right. \\ &\quad \times \left[ \left( \frac{2\ell_p}{L} - 1 \right) + \left( \frac{L}{\ell_p} - 1 \right) A_{L/\ell_p-2}^{L/\ell_p} \left( \frac{L}{\ell_p}, \frac{\Delta_o}{\ell_p} \right) \right. \\ &\quad \left. \left. + A_{L/\ell_p-2}^{L/\ell_p} \left( \frac{L}{\ell_p}, \frac{\Delta_o}{\ell_p} \right) \frac{L}{\ell_p} \left[ 1 + \frac{\Delta_o}{\ell_p} \left( 1 - \frac{L}{\ell_p} \right) \right] \right] \right\}. \end{aligned} \quad (33)$$

#### D. Polymer propagator

Let us now proceed to evaluate the polymer propagator. For this purpose, the starting point is the Fourier transform of the characteristic function which is

$$P(R) = \frac{1}{(2\pi)^3} \int d\mathbf{q} C(q) \exp(-i\mathbf{q}\mathbf{R}). \quad (34)$$

After integrating out the angular variables and using the parity properties of the characteristic function, we can rewrite the integral in Eq. (34) as follows:

$$P(R) = \frac{1}{4\pi^2 R} \int_{-\infty}^{+\infty} dq \sin(qR) q C(q). \quad (35)$$

The change of variables  $t = (2\ell_p^2/L\Delta_o)u$  transforms the expression of the characteristic function given in Eq. (23) in the following way:

$$\begin{aligned} C(q) &= \frac{\Delta_o}{2qz\ell_p^2} \int_0^{+\infty} dt \exp \left( -\frac{t^2}{4} \frac{\Delta_o}{\ell_p} \left( \frac{L}{\ell_p} \right)^2 \right) \\ &\quad \times \operatorname{Im} \left\{ \frac{[\sinh(t+iq\ell_p)]^{L/\ell_p}}{[t+iq\ell_p]^{L/\ell_p-1}} \right\}. \end{aligned} \quad (36)$$

Replacing this integral expression for the characteristic function into the integral representation of the polymer propagator showed in Eq. (35) gives the following result:

$$\begin{aligned} P(R) &= \frac{\Delta_o}{8\pi^2 R z \ell_p^2} \int_0^{+\infty} dt \exp \left[ -\frac{t^2}{4} \frac{\Delta_o}{\ell_p} \left( \frac{L}{\ell_p} \right)^2 \right] \\ &\quad \times \int_{-\infty}^{+\infty} dq \sin(qR) \operatorname{Im} \left\{ \frac{[\sinh(t+iq\ell_p)]^{L/\ell_p}}{[t+iq\ell_p]^{L/\ell_p-1}} \right\}, \end{aligned} \quad (37)$$

which can be rewritten using the Taylor expansion of the function  $\sinh^x(z)$ .<sup>24</sup> The result is

$$\begin{aligned} P(R) &= \frac{\Delta_o}{2^{L/\ell_p+3} \ell_p^{L/\ell_p+1} \pi^2 R z} \sum_{p=0}^{\infty} \binom{L/\ell_p}{p} (-)^p \\ &\quad \times \int_0^{+\infty} dt \exp \left[ -\frac{t^2}{4} \frac{\Delta_o}{\ell_p} \left( \frac{L}{\ell_p} \right)^2 + \left( \frac{L}{\ell_p} - 2p \right) t \right] \\ &\quad \times \operatorname{Im} \left\{ \int_{-\infty}^{+\infty} dq \sin(qR) \frac{\exp \left[ iq\ell_p \left( \frac{L}{\ell_p} - 2p \right) \right]}{[t/\ell_p + iq]^{L/\ell_p-1}} \right\}. \end{aligned} \quad (38)$$

The integral over  $q$  is solvable exactly. Thus, the resulting expression for the propagator is the following:

$$\begin{aligned} P(R) &= \frac{-\Delta_o}{2^{L/\ell_p+3} \ell_p^{L/\ell_p+1} R z \pi \Gamma(L/\ell_p-1)} \left\{ \int_0^{+\infty} dt \exp \left[ -\frac{t^2}{4} \frac{\Delta_o}{\ell_p} \left( \frac{L}{\ell_p} \right)^2 - Rt/\ell_p \right] \sum_{p=0}^{[L+R/2\ell_p]} \binom{L/\ell_p}{p} (-)^p \right. \\ &\quad \times \left[ \ell_p \left( \frac{L}{\ell_p} - 2p \right) + R \right]^{L/\ell_p-2} - \sum_{p=0}^{[L-R/2\ell_p]} \binom{L/\ell_p}{p} (-)^p \left[ \ell_p \left( \frac{L}{\ell_p} - 2p \right) - R \right]^{L/\ell_p-2} \int_0^{+\infty} dt \\ &\quad \left. \times \exp \left[ -\frac{t^2}{4} \frac{\Delta_o}{\ell_p} \left( \frac{L}{\ell_p} \right)^2 + Rt/\ell_p \right] \right\}. \end{aligned} \quad (39)$$

The two integrals present in the expression of the polymer propagator showed in Eq. (39) are exactly solvable. The results are the following:

$$\int_0^{+\infty} dt \exp \left( -\frac{t^2}{4b} \pm at \right) = \sqrt{\pi b} \exp(a^2 b) [1 \pm \operatorname{erf}(a\sqrt{b})] \quad b > 0. \quad (40)$$

Consequently, the final expression for the polymer propagator is given by the following formula:

$$P(R) = - \frac{\Delta_o \sqrt{\frac{\ell_p}{\Delta_o}} \exp\left(\frac{\ell_p R^2}{\Delta_o L^2}\right)}{2^{L/\ell_p+3} \ell_p^2 L z \sqrt{\pi} \Gamma(L/\ell_p - 1)} \left\{ \left[ 1 - \operatorname{erf}\left(\frac{R}{L} \sqrt{\frac{\ell_p}{\Delta_o}}\right) \right]^{[L+R/2\ell_p]} \sum_{p=0}^{[L+R/2\ell_p]} (-)^p \binom{L/\ell_p}{p} \left(\frac{L+R}{\ell_p} - 2p\right)^{L/\ell_p-2} \right. \\ \left. - \left[ 1 + \operatorname{erf}\left(\frac{R}{L} \sqrt{\frac{\ell_p}{\Delta_o}}\right) \right]^{[L-R/2\ell_p]} \sum_{p=0}^{[L-R/2\ell_p]} \binom{L/\ell_p}{p} (-)^p \left(\frac{L-R}{\ell_p} - 2p\right)^{L/\ell_p-2} \right\}, \tag{41}$$

which is valid for any value of the persistence length and contour length of the chain.

**E. Structure factor**

Finally, we compute the single chain structure factor from the well-known formula

$$S(q) = \frac{2}{L^2} \int_0^L ds (L-s) C(q, s). \tag{42}$$

First, we define two dimensionless variables  $s = v \ell_p$  and  $Q = q \ell_p$  where  $\ell_p$  is the true persistence length of the polymer chain. The resulting expression for the structure factor is

$$S(Q) = \frac{2 \ell_p^2}{L^2} \int_0^{L/\ell_p} dv (L/\ell_p - v) C(Q, v). \tag{43}$$

For the purpose of clarity, let us define the ratio  $L/\ell_p = \tau$  in Eq. (43), then the expression of the structure factor becomes

$$S(Q) = \frac{2}{\tau^2} \int_0^\tau dv (\tau - v) C(Q, v), \tag{44}$$

where

$$C(Q, v) = \frac{2}{Q v z(v) 4^{t(v)} \left(\frac{\Lambda_o(v)}{t(v)^2}\right)^{t(v)-1}} \sum_{p=0}^\infty \binom{t(v)}{p} (-)^p \\ \times \operatorname{Im} \left\{ \int_0^{+\infty} du \frac{\exp\left[-u^2 \frac{\Lambda_o(v)}{t(v)} + (t(v) - 2p) \frac{2\Lambda_o(v)}{t(v)^2} \left(u + i Q v \frac{t(v)}{2\Lambda_o(v)}\right)\right]}{\left[u + i Q v \frac{t(v)}{2\Lambda_o(v)}\right]^{t(v)-1}} \right\} \tag{45}$$

and

$$z = z(v) = \left[\frac{t(v)^2}{2\Lambda_o(v)}\right]^2 A_{t(v)-2}^t\left(t(v), \frac{t(v)}{\Lambda_o(v)}\right). \tag{46}$$

We have introduced two new functions of  $v$ , namely  $t(v)$  and  $\Lambda_o(v)$ . The former is equal to the ratio  $L/\ell_p$  used in our solution to the model. We remind the reader that this ratio can differ from the true one, as discussed in Sec. II of this paper. Thus, it should be a function, called  $t(v)$ , of the true value of the ratio  $L/\ell_p$ . The latter function is the ratio  $L/\Delta_o$  used in our calculations. More discussion about these two functions and their explicit mathematical expressions are presented in the following section.

The final expression for the structure factor is obtained by replacing the expressions of  $C(Q, v)$  and  $z(v)$  given in Eqs. (45) and (46) into the integral representation of the structure factor showed in Eq. (44).

**III. RESULTS AND DISCUSSION**

We begin the discussion of our results by considering the two parameters of our approximate treatment of the WLC

model, namely  $\Delta_o$  and  $L/\ell_p$ . Although the physical concepts behind the approximations used to define these parameters were justified in the preceeding section, we now face the problem of determining these parameters quantitatively. For this purpose, we have to define a criterion that should build

TABLE I. List of values used to construct Eqs. (48) and (49).

$\tau$	$t$	$\Lambda_o$
0.1	4.02	454
0.2	4.1	242.5
0.3	4.225	176.5
0.5	4.4	121.5
1	4.8	83.5
10	10	84
12	12	118
15	15	180
18	18	256
20	20	314
25	25	484
35	35	940

TABLE II. Constants for Eq. (48).

Constant	Value
$a_0$	40.9658
$a_1$	42.8935
$a_2$	-6.1775
$a_3$	1.07249
$a_4$	-4.7137E-3

the functional relationships between these two parameters and the parameters used in other approaches to the WLC model.

At this point, one very relevant observation is that our approach targets a generating function that depends on reciprocal space variables ( $\mathbf{q}$ ) explicitly. Consequently, if the approximate mathematical expression for the generating function is accurate then, all the results that depend on reciprocal space variables, such as the single chain structure factor and the characteristic function, will be accurate because they are determined from the generating function directly or through integral operators. This implies that the magnitude of any error made in the evaluation of the generating function will remain the same or be reduced in all statistical properties computed from the generating function that depend on reciprocal space variables. On the contrary, the magnitude of the errors will be magnified by the inverse Fourier transform required to compute real space properties. This leads us to the conclusion that in order to have accurate results for reciprocal and real space statistical quantities, the best way to determine the parameters  $\Delta_o$  and  $L/\ell_p$  is to require that our result for one real space property agrees on a quantitative level with the same real space property predicted by other treatments of the WLC model. Thus, our criterion for the determination of  $\Delta_o$  and  $L/\ell_p$  is that the height and location of the maximum of the radial distribution function for the end-to-end distance agree with the ones obtained from other treatments of the WLC model. For this purpose, we chose two classic results: the work by Gobush *et al.*<sup>10</sup> who calculated the polymer propagator as an expansion around the fully flexible limit and the results obtained by Wilhelm and Frey<sup>21</sup> who studied the rodlike limit.

We start by rewriting our parameters in dimensionless form. We call these parameters  $t$  and  $\Lambda_o$  which are defined as follows:

$$t = L/\ell_p \quad \text{and} \quad \Lambda_o = L/\Delta_o. \tag{47}$$

In addition, we define the variable  $r$  as  $R/L$  where  $R$  is the end-to-end distance. Then, we extract the functional relationship between our new parameters,  $t$  and  $\Lambda_o$ , and the param-

TABLE III. Constants for Eq. (49).

Constant	Value
$b_0$	4.19767
$b_1$	1.9614E-1
$b_2$	5.37968E-2
$b_3$	-1.51054E-3
$b_4$	1.51895E-5

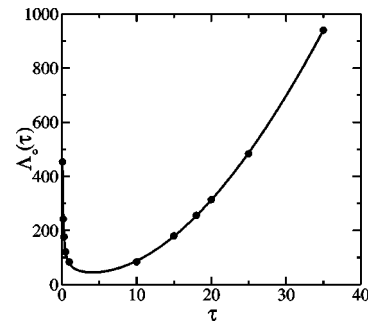


FIG. 2. Plot of  $\Lambda_o(\tau)$  vs  $\tau$ . Continuous line [least squares fit from Eq. (48)], circles (numerical values from Table I).

eter  $\tau$ , defined as the *true* ratio  $L/\ell_p$ , by matching the position and height of the peak in the radial distribution function of the end-to-end distance [ $4\pi r^2 P(r)$ ] obtained by using our method with the ones obtained from the studies of Gobush *et al.*<sup>10</sup> and Wilhelm and Frey.<sup>21</sup> Table I shows the values obtained from the fitting procedure and, Eqs. (48) and (49) are the least square fits to these data points,

$$\Lambda_o(\tau) = \frac{a_0}{\tau} + a_1 + a_2\tau + a_3\tau^2 + a_4\tau^3, \tag{48}$$

$$t(\tau) = b_0 + b_1\tau + b_2\tau^2 + b_3\tau^3 + b_4\tau^4, \tag{49}$$

where the values of the coefficients are given in Tables II and III. Equations (48) and (49) are valid for values of  $\tau$  in the interval  $[0.1, 40]$ . However, these fits can be extended to any value of  $\tau$  using the procedure described before. For the purpose of illustration we plotted Eqs. (48) and (49) in Figs. 2 and 3, respectively. Both figures display very good quantitative agreement between the data and the least square fits. Consequently, Eqs. (48) and (49) can be used to make predictions for the polymer propagator for intermediate values of  $\tau$ .

The dependence of  $\Lambda_o(\tau)$  on  $\tau$  is showed in Fig. 2. Observe that  $\Lambda_o(\tau)$  decreases with increasing  $\tau$  for small values of  $\tau$ . This implies that as the chain becomes shorter, the self-correlations become weaker. This is a clear consequence of the kernel  $K_{k,s}$  which approaches zero for short chains because it is proportional to  $|s-k|$ . On the other hand,  $\Lambda_o(\tau)$  increases with increasing  $\tau$  for large values of  $\tau$  (long chains) which implies that the self-correlations become weaker. This is the natural consequence of the fact that, in

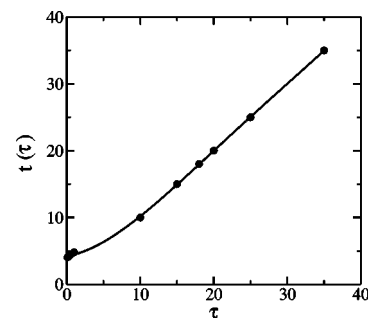


FIG. 3. Plot of  $t(\tau)$  vs  $\tau$ . Continuous line [least squares fit from Eq. (49)], circles (numerical values from Table I).

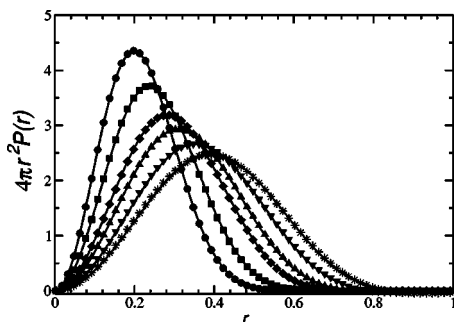


FIG. 4. Normalized radial distribution function,  $4\pi r^2 P(r)$ , vs  $r$ . Comparison between our results (continuous lines), Eq. (41), and Gobush's results (symbols) for the following values of  $\tau$ : 35 (circles), 25 (squares), 18 (diamonds), 15 (triangles up), 12 (triangles down), and 10 (stars).

this limit, the chain is in the flexible regime. Thus, all the effects that are consequences of the semiflexible nature of the polymer backbone become negligible. Therefore,  $\Lambda_o(\tau)$  displays a minimum for values of  $\tau$  close to four. The dependence of  $t(\tau)$  on  $\tau$  is showed in Fig. 3. This plot shows the expected monotonic behavior. Furthermore, for large enough values of  $\tau$ , the relationship is linear. This result can be rationalized as follows: the longer the chain is, the less important the fluctuations around the rodlike configuration (for *one* persistence length) are. Thus, our  $L/\ell_p$  should approach the true value of  $L/\ell_p$  as the chain becomes longer.

Let us now turn the attention to the polymer propagator  $P(R)$  whose expression is showed in Eq. (41). It is worth observing that apart from some prefactors, the dependence of the propagator on  $R$  is mathematically very simple. It is just the sum of two terms each of which is the product of an exponential, a term involving an error function and a *finite* sum of powers. Considering that this expression was derived from the characteristic function, Eq. (36), via an inverse Fourier transform, we find this expression to be remarkably simple.

Figure 4 shows the radial distribution function [ $4\pi r^2 P(r)$ ] predicted by our calculations using Eqs. (48) and (49), and the one predicted using the expression derived by Gobush *et al.*<sup>10</sup> Both results are in excellent quantitative agreement. Figure 5 shows the same quantity near the rodlike limit. In this case, we compare our results with the ones obtained in Ref. 21. As in the previous case, the quantitative

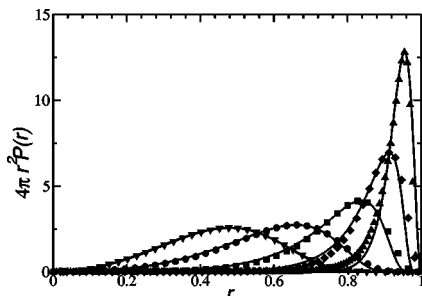


FIG. 5. Normalized radial distribution function,  $4\pi r^2 P(r)$ , vs  $r$ . Comparison between our results (continuous lines), Eq. (41), and Frey's results (symbols) for the following values of  $\tau$ : 10 (triangles down), 5 (circles), 2 (squares), 1 (diamonds), and 0.5 (triangles up).

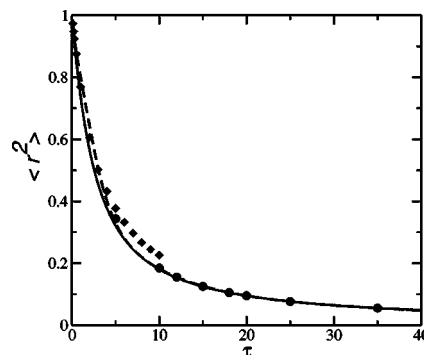


FIG. 6. Mean square end-to-end distance (divided by  $L^2$ )  $\langle R^2 \rangle$  vs the parameter  $\tau$ . Our result (dashed line), exact result (solid line), Ref. 10 (circle) and Ref. 21 (diamonds).

agreement is very good for all the values of  $\tau$  studied. The small deviations observed between both results can be corrected in a perturbative way as described in the preceding section. It is important to observe that the results for the radial distribution function arising from Refs. 10 and 21 disagree for  $\tau=10$ . But, independently of which one is the most accurate one, our method can be made to agree with it by the appropriate selection of the values of  $\Lambda_o$  and  $t$ .

Figures 4 and 5 also show how both asymptotic behaviors are connected. The location of the peak in our radial distribution function for chains with a fixed contour length,  $L$ , moves toward larger values of  $r$  when the persistence length  $\ell_p$  of the polymer backbone increases. This is the correct result because the stiffer the polymer backbone, the higher the energetic penalty to bend the chain. Consequently, those configurations of the macromolecule with small end-to-end distance will be more and more hindered as the persistence length increases, while those configurations with large end-to-end distance should be more favored. Therefore, the peak shifts toward larger values of  $r$  when the persistence length increases. Moreover, the height of the peak must increase to preserve the normalization of the radial distribution function.

Figure 6 shows four different results for the mean square end-to-end distance (divided by  $L^2$ ). Our result which is represented by the dashed line was obtained by replacing the expressions of  $\Lambda_o(\tau)$  and  $t(\tau)$  showed in Eqs. (48) and (49) into the mathematical formula for  $\langle R^2 \rangle$  given by Eq. (33). The solid line corresponds to the exact solution.<sup>2</sup> The circles

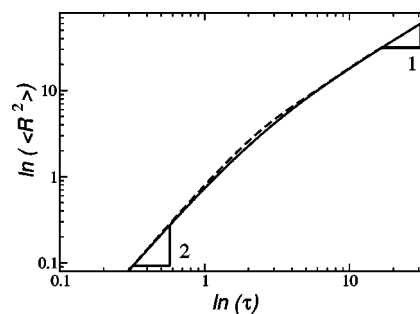


FIG. 7. Same data as in Fig. 6 plotted differently (only two data sets are showed). Our result (dashed line) and exact result (solid line).

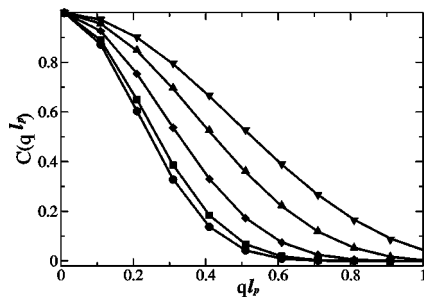


FIG. 8. Characteristic function  $C(q)$ , Eq. (26), vs wave vector  $q$ . Continuous lines this work, symbols Stepanow and Schütz ( $L^{-1}[G_{10}(k,p)](k,\tau)$  in their notation). Circles ( $\tau=35$ ), squares ( $\tau=30$ ), diamonds ( $\tau=20$ ), triangles up ( $\tau=12$ ), and triangles down ( $\tau=8$ ).

and diamonds correspond to the mean square end-to-end distance obtained from Refs. 10 and 21, respectively. This figure shows that our result is in very good quantitative agreement with the exact result over the whole range of values of  $\tau$ . In particular, it captures the fractal dimensions of the flexible and rigid limits correctly, as showed in Fig. 7.

Let us now consider reciprocal space quantities. For this purpose, we start with the characteristic function  $C(q)$ . Figures 8 and 9 show  $C(q)$  as a function of  $q$  for ten different values of  $\tau$  (0.1,0.5,1,2,4,8,12,20,30, and 35). The symbols are the results obtained using the method of Stepanow and Schütz for  $n=10$  (in their notation).<sup>23</sup> These figures clearly show that our results capture the continuous change in the behavior of this function which changes from a monotonically decreasing function in the flexible limit (large values of  $\tau$ ) to an oscillating function in the rodlike regime (small values of  $\tau$ ). In addition, our computations predict that, for a fixed  $l_p$ , the decrease of the characteristic function for small values of  $q$  should be faster for flexible polymers than for rigid ones. This is a consequence of the fact that for a fixed persistence length the flexible limit is achieved with large contour lengths thus, the mean square end-to-end distance is larger and the decrease in the characteristic function is more pronounced than in the rigid limit which is realized by short contour lengths thus, small mean square end-to-end distances. In addition, Figs. 8 and 9 show that the results obtained using our method can describe reciprocal space properties accurately.

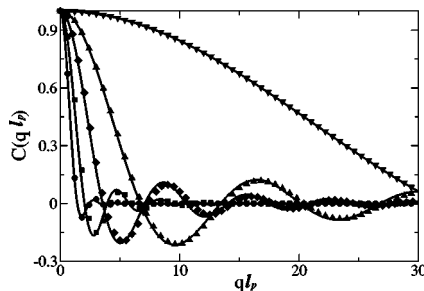


FIG. 9. Characteristic function  $C(q)$ , Eq. (26), vs wave vector  $q$ . Continuous lines this work, symbols Stepanow and Schütz ( $L^{-1}[G_{10}(k,p)](k,\tau)$  in their notation). Circles ( $\tau=4$ ), squares ( $\tau=2$ ), diamonds ( $\tau=1$ ), triangles up ( $\tau=0.5$ ), and triangles down ( $\tau=0.1$ ).

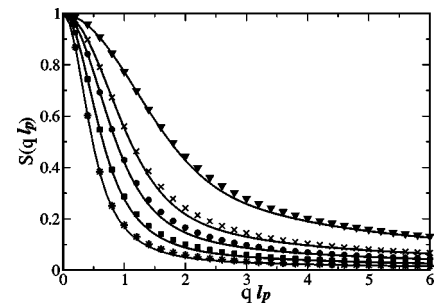


FIG. 10. Structure factor  $S(q)$  vs wave vector  $q$ . Comparison of our results (continuous lines), Eq. (44), with Kholodenko's results (symbols). Stars ( $\tau=35$ ), squares ( $\tau=20$ ), circles ( $\tau=12$ ),  $\times$  ( $\tau=8$ ), and triangles ( $\tau=4$ ).

Based on the aforementioned expression for the characteristic function, we have also computed the single chain structure factor  $S(q)$  whose final expression is showed in Eq. (44). Furthermore, we have compared it with the prediction arising from the model for semiflexible (Dirac) chains developed by Kholodenko<sup>5</sup> which was successfully tested against experimental data<sup>27</sup> and Monte Carlo simulations based on a discrete form of the Kratky–Porod model for worm-like chains.<sup>28</sup> We present this comparison in Figs. 10 and 11 where we plotted  $S(q)$  as a function of  $q$  for nine different values of the persistence length. The symbols correspond to Kholodenko's model and the lines are the results of our calculations. These figures depict an excellent quantitative agreement between both results for the whole range of values of  $\tau$  studied. This agreement is to be expected due to the approximate equivalence, via the Bloch–Nordsieck approximation, between the WLC model and the model of Dirac chains. The observed quantitative agreement between our *approximate* results and the exact ones for Dirac chains implies that our approximation to the WLC model is accurate and the use of an effective self-correlation does not affect the predicted  $S(q)$  significantly.

#### IV. CONCLUSIONS

In this article we have developed a new approach to the WLC model of semiflexible polymers based on a new generating function. The advantage of our approach is fivefold. First, the evaluation of the most relevant statistical properties of the model is straight forward since they can be obtained as derivatives or integrals of the generating function. This

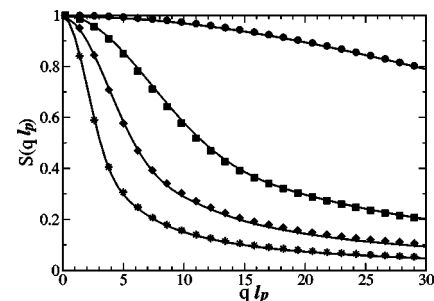


FIG. 11. Structure factor  $S(q)$  vs wave vector  $q$ . Comparison of our results (continuous lines), Eq. (44), with Kholodenko's results (symbols). Stars ( $\tau=2$ ), diamonds ( $\tau=1$ ), squares ( $\tau=0.5$ ), and circles ( $\tau=0.1$ ).

makes the evaluation of the generating function the fundamental step for the solution of the WLC model. In our treatment of the model, we devised two approximations that were able to capture the flexible and rigid limits exactly and, moreover, provided a smooth crossover behavior between the two aforementioned limiting regimes. This crossover behavior has all the correct qualitative features as showed in the preceding section and, furthermore, agrees on a quantitative level with the results obtained by five other research groups. Second, all the results obtained using our method are based on the same approximations. In other words, there is no need to develop different approximations for different statistical properties or regimes with different degrees of stiffness. This puts all our results on equal footing. Third, our method provides closed form mathematical expressions for all the properties studied in this paper. Some of these expressions, like the one of the polymer propagator in real space, turned out to be very simple. Fourth, another important advantage of this work is that it respects the local, not global, inextensibility constraint. Consequently, this method could be used to study the force-elongation relationship of worm-like polymers. We will study this topic in a future note. Finally, our treatment of the WLC model was able to provide a solution to this model around which a standard perturbative treatment can be developed. In this paper we did not pursue the development of such perturbative treatment. However, we provided the guidelines for it. The detailed calculations will be the topic of a future publication.

Perhaps, one of the most important contributions of our work is the derived polymer propagator. The mathematical expression obtained for the propagator is very simple. It contains two terms each of which is the product of an exponential, a term which involves an error function and a finite sum of powers which is very similar to the expression of the polymer propagator of the random flight model.

## ACKNOWLEDGMENTS

This paper is based upon work supported by the National Science Foundation under Grant No. CHE-0132278. Also, acknowledgment is made to The Ohio Board of Regents, Action Fund (Grant No. R566), and The University of Akron for financial support.

## APPENDIX: SOME MATHEMATICAL ASPECTS OF THE EVALUATION OF THE GENERATING FUNCTION

In this Appendix we explain how the final expression of the generating function, Eq. (11), was obtained. For the purpose of clarity we define the variables  $\{Y_k\}$  as follows:

$$Y_k \equiv [i\Phi_k(1 + \lambda_q) + \Psi_{kjp}], \quad (\text{A1})$$

then, the integrals over the variables  $u_k$  in Eq. (8) can be evaluated exactly using the saddle point method which is the solution to the following equations:

$$\mathbf{u}_1 - \mathbf{u}_0 = -\kappa Y_0, \quad (\text{A2})$$

$$\mathbf{u}_{n-1} - \mathbf{u}_{n-2} = \kappa Y_{n-1}, \quad (\text{A3})$$

$$\mathbf{u}_{k+1} - 2\mathbf{u}_k + \mathbf{u}_{k-1} = -\kappa Y_k, \quad k = 1 \dots n-2, \quad (\text{A4})$$

where  $\kappa$  was defined in Eq. (12). The solutions to these equations are given in Eq. (9). Moreover, the constraint stated in Eq. (10) is a consequence of these equations. Therefore, if this constraint is not satisfied, then Eq. (9) is not the saddle point solution.

The terms appearing in Eq. (8) can be rewritten as follows:

$$-\frac{1}{2\kappa} \sum_{k=0}^{n-2} (\mathbf{u}_{k+1} - \mathbf{u}_k)^2 = -\frac{\kappa}{2} \sum_{k=0}^{n-2} \left( \sum_{m=0}^k Y_m \right)^2, \quad (\text{A5})$$

and also

$$\sum_{k=0}^{n-1} \mathbf{u}_k \cdot Y_k = -\frac{\kappa}{2} \sum_{k=0}^{n-1} \sum_{m=0}^{n-1} Y_m |k-m| Y_k. \quad (\text{A6})$$

We can simplify the sum of these two terms further if we note that

$$\begin{aligned} & \sum_{k=0}^{n-1} \sum_{m=0}^{n-1} Y_m |k-m| Y_k + \sum_{k=0}^{n-2} \left( \sum_{m=0}^k Y_m \right)^2 \\ &= \sum_{k=0}^{n-1} \sum_{m=0}^{n-1} Y_m |k-m| Y_k + \sum_{k=0}^{n-2} \sum_{m=0}^k Y_m Y_k (n-1-k) \\ & \quad + \sum_{k=0}^{n-2} \sum_{m=k+1}^{n-1} Y_m Y_k (n-1-m) \\ &= \sum_{k=0}^{n-1} \sum_{m=0}^{n-1} Y_m |k-m| Y_k - \sum_{k=0}^{n-2} \sum_{m=k+1}^{n-1} Y_m (m-k) Y_k \\ & \quad + (n-1) \sum_{k=0}^{n-2} \sum_{m=0}^{n-1} Y_m Y_k, \end{aligned} \quad (\text{A7})$$

where the last double sum vanishes because of the constraint given by Eq. (10). After changing the order of summation we obtain the following expression:

$$\sum_{k=0}^{n-1} \sum_{m=0}^{n-1} Y_m |k-m| Y_k - \sum_{k=1}^{n-1} \sum_{m=0}^{k-1} Y_m (k-m) Y_k. \quad (\text{A8})$$

Apart from the term  $k=0$  the first double sum can be separated into two terms: one for  $m \leq k-1$  and the other one for  $m \geq k$  such that the former cancels the second double sum in the preceding expression. As a result we obtain

$$\begin{aligned} & \sum_{k=0}^{n-1} Y_0 k Y_k + \sum_{k=1}^{n-1} \sum_{m=k}^{n-1} Y_m |k-m| Y_k \\ &= \sum_{k=0}^{n-1} \sum_{m=0}^{n-1} Y_m (m-k) \Theta(m-k) Y_k. \end{aligned} \quad (\text{A9})$$

If we now use the constraint for the  $Y_k$ 's, Eq. (10), we obtain the quadratic term in Eq. (11).

<sup>1</sup>G. Porod, *Monatsch. Chem.* **80**, 251 (1949); O. Kratky and G. Porod, *Recl. Trav. Chim. Pays-Bas* **68**, 1106 (1949).

<sup>2</sup>N. Saitô, K. Takahashi, and Y. Yunoki, *J. Phys. Soc. Jpn.* **22**, 219 (1967).

<sup>3</sup>H. Yamakawa, *Helical Worm-like Chains in Polymer Solutions* (Springer, Berlin, 1997).

<sup>4</sup>H. Kleinert, *Path Integrals in Quantum Mechanics, Statistics, Polymer Physics, and Financial Markets* (World Scientific, Singapore, 2003).

<sup>5</sup>A. L. Kholodenko, *Phys. Lett. A* **141**, 351 (1989); *Ann. Phys.* **202**, 186

- (1990); Phys. Lett. A **178**, 180 (1993); Macromolecules **26**, 4179 (1993); A. Kholodenko and T. Vilgis, Phys. Rev. E **50**, 1257 (1994); J. Chem. Soc., Faraday Trans. **91**, 2473 (1995); A. L. Kholodenko and T. A. Vilgis, Phys. Rev. E **52**, 3973 (1995); A. Kholodenko, M. Ballauff, and M. Aguero, Physica A **260**, 267 (1998).
- <sup>6</sup>H. E. Daniels, Proc. Roy. Soc. Edinburgh **A63**, 290 (1952).
- <sup>7</sup>H. Benoit and P. Doty, J. Phys. Chem. **57**, 958 (1953).
- <sup>8</sup>M. Fixman and J. Kovac, J. Chem. Phys. **58**, 1564 (1973).
- <sup>9</sup>R. A. Harris and J. E. Hearst, J. Chem. Phys. **44**, 2595 (1966).
- <sup>10</sup>W. Gobush, H. Yamakawa, W. H. Stockmayer, and W. S. Magee, J. Chem. Phys. **57**, 2839 (1972).
- <sup>11</sup>H. Yamakawa and W. H. Stockmayer, J. Chem. Phys. **57**, 2843 (1972).
- <sup>12</sup>K. F. Freed, in *Advances in Chemical Physics*, edited by I. Prigogine and S. A. Rice (Wiley, New York, 1972), Vol. 22, pp. 1–128.
- <sup>13</sup>M. G. Bawendi and K. F. Freed, J. Chem. Phys. **83**, 2491 (1985).
- <sup>14</sup>J. B. Lagowski, J. Noolandi, and B. Nickel, J. Chem. Phys. **95**, 1266 (1991).
- <sup>15</sup>R. G. Winkler, P. Reineker, and L. Harnau, J. Chem. Phys. **101**, 8119 (1994).
- <sup>16</sup>S. R. Zhao, C. P. Sun, and W. X. Zhang, J. Chem. Phys. **106**, 2520 (1997).
- <sup>17</sup>S. M. Bhattacharjee and M. Muthukumar, J. Chem. Phys. **86**, 411 (1987).
- <sup>18</sup>M. G. Poirier *et al.*, Phys. Rev. Lett. **86**, 360 (2001); J. F. Leger *et al.*, *ibid.* **83**, 1066 (1999); V. Parpura and J. M. Fernandez, Biophys. J. **71**, 2356 (1996); M. D. Wang *et al.*, *ibid.* **72**, 1335 (1997); A. D. Mehta, K. A. Pullen, and A. Spudich, FEBS Lett. **430**, 23 (1998); A. D. Mehta, M. Rief, and J. A. Spudich, J. Biol. Chem. **274**, 14517 (1999); T. E. Fisher, P. E. Marszalek, and J. M. Fernandez, Nat. Struct. Biol. **7**, 719 (2000); T. E. Fisher *et al.*, Trends Biochem. Sci. **24**, 379 (1999); M. Carrion-Vazquez *et al.*, Prog. Biophys. Mol. Biol. **74**, 63 (2000); T. T. Perkins, S. R. Quake, D. E. Smith, and S. Chu, Science **264**, 822 (1994); S. B. Smith, Y. Cui, and C. Bustamante, *ibid.* **271**, 795 (1996); T. T. Perkins, D. E. Smith, and S. Chu, *ibid.* **276**, 2016 (1997); A. F. Oberhauser, P. E. Marszalek, H. P. Erickson, and J. M. Fernandez, Nature (London) **393**, 181 (1998); F. Oesterhelt, M. Rief, and H. E. Gaub, New J. Phys. **1**, 6.1 (1999); H. B. Li, W. K. Zhang, W. Q. Xu, and X. Zhang, Macromolecules **33**, 465 (2000).
- <sup>19</sup>J. F. Marko and E. D. Siggia, Macromolecules **28**, 8759 (1995); K. Kroy and E. Frey, Phys. Rev. Lett. **77**, 306 (1996); J. Samuel and S. Sinha, Phys. Rev. E **66**, 050801 (2002).
- <sup>20</sup>P. L. Hansen and R. Podgornik, J. Chem. Phys. **114**, 8637 (2001).
- <sup>21</sup>J. Wilhelm and E. Frey, Phys. Rev. Lett. **77**, 2581 (1996).
- <sup>22</sup>R. G. Winkler, J. Chem. Phys. **118**, 2919 (2003).
- <sup>23</sup>S. Stepanow and G. M. Schütz, Europhys. Lett. **60**, 546 (2002).
- <sup>24</sup>I. S. Gradshteyn and I. M. Ryzhik, *Table of Integrals, Series, and Products* (Academic, New York, 2000).
- <sup>25</sup>H. Yamakawa, *Modern Theory of Polymer Solutions* (Harper & Row, New York, 1971); M. Marucho and G. A. Carri, J. Math. Phys. **44**, 6020 (2003).
- <sup>26</sup>J. S. Higgins and H. C. Benoit, *Polymers and Neutron Scattering* (Clarendon, Oxford, 1996).
- <sup>27</sup>P. Hickl, M. Ballauff, U. Scherf, K. Mullen, and P. Lindher, Macromolecules **30**, 273 (1997).
- <sup>28</sup>D. Pötschke, P. Hickl, M. Ballauff, P. O. Åstrand, and J. S. Pedersen, Macromol. Theory Simul. **9**, 345 (2000).